Available online at www.sciencedirect.com

ScienceDirect

journal homepage: www.jfda-online.com

Review Article

Nanomaterial-based sensors for detection of foodborne bacterial pathogens and toxins as well as pork adulteration in meat products

B. Stephen Inbaraj, B.H. Chen *

Department of Food Science, Fu Jen Catholic University, Taipei, Taiwan

ARTICLE INFO

Article history:
Received 9 March 2015
Received in revised form
22 April 2015
Accepted 8 May 2015
Available online 26 July 2015

Keywords:
bacterial pathogens
food analysis
food toxins
nanomaterials
pork adulteration

ABSTRACT

Food safety draws considerable attention in the modern pace of the world owing to rapid-changing food recipes and food habits. Foodborne illnesses associated with pathogens, toxins, and other contaminants pose serious threat to human health. Besides, a large amount of money is spent on both analyses and control measures, which causes significant loss to the food industry. Conventional detection methods for bacterial pathogens and toxins are time consuming and laborious, requiring certain sophisticated instruments and trained personnel. In recent years, nanotechnology has emerged as a promising field for solving food safety issues in terms of detecting contaminants, enabling controlled release of preservatives to extend the shelf life of foods, and improving food-packaging strategies. Nanomaterials including metal oxide and metal nanoparticles, carbon nanotubes, and quantum dots are gaining a prominent role in the design of sensors and biosensors for food analysis. In this review, various nanomaterial-based sensors reported in the literature for detection of several foodborne bacterial pathogens and toxins are summarized highlighting their principles, advantages, and limitations in terms of simplicity, sensitivity, and multiplexing capability. In addition, the application through a noncross-linking method without the need for any surface modification is also presented for detection of pork adulteration in meat products.

1. Introduction

Foodborne diseases are caused by consuming foods or beverages contaminated by bacteria, viruses, and parasites. The worldwide statistics on foodborne diseases published for 2011–2012 by the Centers for Disease Control and Prevention reported a total of 1632 outbreaks, 29,112 affected patients, 1750 hospitalizations, and 68 deaths [1]. Some of the various bacterial pathogens that cause foodborne diseases and eventual death are *Salmonella* (31%), *Listeria* (28%), *Campylobacter* (5%), and *Escherichia coli* O157:H7 (3%) [1,2]. Likewise, the trend

* *Corresponding author*. Department of Food Science, Fu Jen Catholic University, No. 510, Zhongzheng Road, Xinzhuang District, New Taipei City 24205, Taiwan.
E-mail address: 002622@mail.fju.edu.tw (B.H. Chen).

http://dx.doi.org/10.1016/j.jfda.2015.05.001

of foodborne disease outbreaks in Taiwan between 1991 and 2010 reported by the Food and Drug Administration of Department of Health in Taiwan indicated 4284 outbreaks and 82,342 cases, with annual average number of 285 outbreaks during 2001–2010 being substantially greater than that of 143 during 1991–2000 [3]. The three most common foodborne pathogens responsible for these outbreaks in Taiwan include *Vibrio parahaemolyticus*, *Staphylococcus aureus*, and *Bacillus cereus* [3]. The spread of foodborne disease due to pathogens and toxins causes a substantial loss to the food industry because a large amount of money will be spent on analyzing and identifying preventive measures for food protection [4,5]. Thus, the development of a rapid, sensitive, specific, and cost-effective analytical method is of great importance for detection of microbial contaminants.

Conventional methods for detecting pathogens include microscopy-, nucleic acid-, and immunoassay-based techniques. The microscopy-based methods require a large amount of sample, long incubation time, and tedious culture preparations [6]. However, the discovery of DNA and development of polymerase chain reaction (PCR) have led microbiologists to target genes and proteins instead of the microorganism itself. Although the PCR-based techniques and several other molecular diagnostic methods such as rapid-PCR, ligand chain reaction, checkerboard hybridization, ligase chain reaction, ribotyping, and pulsed-field gel electrophoresis are highly sensitive and selective, they require undamaged DNA, experienced personnel, and expensive equipment as well as reagents, thus making the overall cost of detection high enough to prevent wide-scale application, especially in developing nations and point-of-care scenario [6,7]. The immunoassays involving targeting of specific proteins or carbohydrate moieties to pathogens include enzyme-linked immunosorbent assays (ELISAs) and Western blot analyses, both of which are sensitive and can provide molecular fingerprints of the pathogen. Despite their sensitivity, both ELISA and PCR require extensive sample preparation and long readout time, which can delay the pathogen detection and immediate preventive action toward the infected patients [4,6–8].

Similarly, the toxins secreted by bacteria can induce cytotoxicity by altering the physiological activity and integrity of the plasma membrane [6,7,9]. For example, the Shiga toxin secreted by *E. coli* O157:H7 can inhibit protein synthesis and activate apoptosis and necrosis, whereas listeriolysin O secreted by *Listeria monocytogenes* can create pores for subsequent disruption of the phospholipid bilayer and eventual cell lysis [6,7,9,10]. Although toxins are not usually transmitted through infected individuals, they are able to cause significant devastating effects on organs and tissues. Besides, the toxins can remain in the food, environmental, and clinical samples even after the death of their corresponding pathogens. Therefore, prompt screening of toxins is highly essential to minimize intoxication. Similar to pathogens, the existing detection methods for toxins include ELISA, Western blots, surface plasmon resonance (SPR) biosensors, antibody microarrays, and antibody-coated polystyrene microbeads, all of which are sensitive and possess multiplexing capability [2,4–7,9]. However, these methods are time consuming and laborious, besides requiring homogeneous or purified samples. Furthermore, as these methods are performed in the fluorometric or spectrophotometric mode, the number of samples screened can be limited [2,4–7,9]. Nevertheless, these limitations can be overcome by some other toxin detection techniques such as liquid chromatography-mass spectrometry and multidimensional protein identification [6]. Yet, the requirement of sophisticated instrumentation as well as lack of portability and user friendliness still limits their wide-scale application. Thus, the development of an advanced detection method with nanomaterials as a platform is crucial.

Meatball is a special type of restructured and pulverized meat product, which is popular in many Asian and European countries [11,12]. Pork has been identified as a potential adulterant in beef and chicken meatballs because of cheaper cost [11,13]. Moreover, from the religious and health point of view, the mixing of pork or pork-related products in food raises serious concerns due to violation of Kosher and Halal food laws [12–14]. In addition, consumption of food products with pork adulteration has been reported to cause allergic reactions [10–12], and consumption of these foods at high levels can cause accumulation of cholesterol and saturated fats in the human body, resulting in chronic diseases such as diabetes and cardiovascular disease [11–14]. Thus, the development of a sensitive and selective analytical method is imperative for detection of pork adulteration in meatball preparations.

Recent developments in the field of nanotechnology offer many technological advances for detection of foodborne pathogens and toxins as well as adulteration among meat formulations [2,4–6,9,11–14]. However, most of the published articles have mainly dealt with the theranostic application of nanomaterials for cancer detection and treatment [15]. Owing to the presence of unique properties in nanoscale materials, the sensing devices can be designed to enhance sensitivity, reduce detection time, and enable multiplexing capability [16–18]. Compared with their bulk counterparts, the nano-sized materials (1–100 nm) possess large surface area, exhibit quantum confinement effects, as well as enhance surface reactivity, electrical conductivity, and magnetic properties [6,18]. Most importantly, the properties of nanomaterials can be tailored by changing the size, shape, composition, and modifying the nanomaterial surface with appropriate functionalization. In view of this, the electronic, spectroscopic, light-scattering, and conductive properties can be modified by engineering the structural parameters of nanomaterials including size, composition, self-assembling, and binding [2–6,16–18]. In addition, the groundbreaking developments in surface patterning techniques have paved the way for generating nanoscale arrays for pathogen-targeting ligands, which can drastically improve the accuracy of analytical techniques associated with detection of food-related toxins [6,16,17]. In addition, the application of nanoparticles as sensors in conjugation with affinity ligands, antibodies, as well as the existing novel detection techniques has led to improved sensitivity for simultaneous detection of multiple toxins [2,4–6,16–18]. Several nanomaterials commonly used for detection of foodborne pathogens and toxins include gold nanoparticles (GNPs), gold nanorods, magnetic nanoparticles (MNPs), quantum dots (QDs), silver nanoparticles (SNPs), and silica nanoparticles [2,4,5]. Detection of foodborne pathogens

and toxins is usually achieved by exploiting the optical (optical sensors) or electronic (electrochemical sensors) properties of the nanomaterial [4]. In this review, we have highlighted the application of several nanomaterials as sensors for detection of foodborne bacterial pathogens and toxins. In addition, the application of a promising noncross-linking method requiring no surface modification of nanomaterials used for detection of pork adulteration in meat products is also presented.

2. Nanomaterial-based sensors for bacterial pathogens

Table 1 summarizes a collection of some reported studies on nanomaterial-based sensors used for detection of bacterial pathogens.

2.1. *Escherichia coli*

E. coli O157:H7 is the most important serotype among *E. coli* strains. It has drawn considerable attention owing to its toxin-producing capability, thereby damaging the intestinal lining and causing anemia, stomach cramps, hemolytic uremic syndrome, and hemorrhagic colitis with an infective dose as low as 100 cells [9]. It can be transmitted to humans through consumption of raw or undercooked ground meat products and raw milk. More specifically, several foods reported to be responsible for outbreaks of *E. coli* O157:H7 include undercooked hamburgers, dried cured salami, unpasteurized fresh-pressed apple cider, yogurt, and cheese made from raw milk [4]. In addition, the cross-contamination through feces in water, meat products, fruits, and vegetables has also contributed to *E. coli* O157:H7 outbreaks [4,9]. For the nanoparticle-based detection of *E. coli* O157:H7, Mao et al [19] developed a quartz crystal microbalance (QCM) DNA sensor using streptavidin-conjugated MNPs as mass enhancers to amplify the frequency change. A thiolated single-stranded DNA probe specific to the *E. coli* O157:H7 *eae*A gene was self-assembled onto the QCM sensor followed by inducing hybridization through exposure of this single-stranded DNA probe to the complementary target DNA and amplification using asymmetric PCR with biotin-labeled primers. This resulted in a change in mass with a concomitant change in QCM frequency for detection of *E. coli* O157:H7. The detection limit obtained was 2.67×10^2 colony forming units (CFU)/mL in the linear working range of 2.67×10^2–2.67×10^6 CFU/mL [19]. Based on a similar approach, a circulating-flow piezoelectric biosensor (PEB) was developed for detection of *E. coli* O157:H7 using GNPs-conjugated thiolated probe as mass enhancer and sequence verifier [20]. An *E. coli* O157:H7 *eae*A gene-specific thiolated probe conjugated to PEB was exposed to *E. coli* gene fragment amplified by PCR and the resultant mass change was measured as frequency shift of PEB, with the detection limit obtained being 1.2×10^2 CFU/mL in the linear working range of 10^2–10^6 CFU/mL [20].

For detection of *E. coli* O157:H7 in milk, a disposable immunosensing strip containing double antibodies for indirect sandwich enzyme-linked immunoassay was fabricated by attaching 13-nm GNPs onto screen-printed carbon electrodes (SPCEs) [21]. The electrode was coupled with the first *E. coli* O157:H7-specific antibody, *E. coli* O157:H7 intact cells and the second *E. coli* O157:H7-specific antibody conjugated with horseradish. The hydrogen peroxide and ferrocenedicarboxylic acid (FeDC) were used as a substrate and mediator, respectively. The presence of GNPs and FeDC enhanced the response current by 13.1-folds, allowing for detection of 6 CFU/strip and 50 CFU/strip in buffer and milk, respectively. The concentration range from 10^2 CFU/mL to 10^7 CFU/mL could be detected by this amperometric method. Cho et al [22] developed an electrochemical immunosensor based on deposition of peptide nanotubes on SPCE (PNs–SPCE). The anti-*E. coli* O157:H7 antibody immobilized on PN–SPCE adsorbed *E. coli* O157:H7 from samples through antigen–antibody interaction and the response current was measured by cyclic voltammetry. Some other *E. coli* strains were also detected using sensors incorporating nanomaterials such as MNPs [23], SNPs [24], GNPs [25], and carbon nanotubes (CNTs) [26]. With D-mannose-functionalized MNPs, El-Boubbou et al [23] developed a method to detect *E. coli* cells at 10^4 cells/mL through incubation of the modified MNPs with fluorescein-labeled concanavalin A at 4°C for 12 hours, followed by further incubation with *E. coli* cells in phosphate-buffered saline (PBS) buffer, separation using magnetic field, staining with fluorescent dye, and imaging with epifluorescent microscopy. In a similar study, Kalele et al [24] used rabbit immunoglobulin G (IgG) antibody-conjugated silver nanoshells for rapid and highly selective detection of *E. coli* in the range of 5–10^9 cells by monitoring the change in the SPR band shift in the presence of *E. coli* cells. In addition, a rapid anodic stripping voltammetric detection of *E. coli* using core-shell Cu@GNPs as anti-*E. coli* sensors was also reported [25]. More recently, Maurer et al [26] developed a novel nanobiosensor platform through decoration of CNTs with RNA-coated GNPs for the selective detection of *E. coli*.

2.2. *Salmonella*

Salmonellosis is one of the most important bacterial diseases caused mainly by *Salmonella* species such as *Salmonella enteritidis* and *Salmonella typhimurium* [4]. The WHO statistics reveal about tens of millions of new human cases affected and 100,000 deaths every year, with symptoms including fever, abdominal pain, diarrhea, nausea, and vomiting [2,4,9]. A highly sensitive electrochemical immunoassay for determination of *S. typhimurium* was demonstrated by Dungchai et al [27], who immobilized monoclonal antibodies on polystyrene for capturing bacteria followed by adding polyclonal antibody–GNPs conjugate to bind the bacteria in the presence of copper-enhancer solution and ascorbic acid. The copper released upon reduction was deposited on GNPs for direct measurement of *S. typhimurium* concentration by anodic stripping voltammetry, with the limit of detection being 98.9 CFU/mL and the anodic current linearly depending on *S. typhimurium* concentration over a working range of 1.30×10^2–2.6×10^3 CFU/mL [27]. In a later study, a reusable capacitive immunosensor involving ethylenediamine and GNPs grafted on glass carbon electrode was developed for detection of *Salmonella* spp. in commercial pork samples [28]. The interaction of monoclonal antibody–GNPs conjugated

Table 1 – Some reported nanomaterial-based sensors for detection of different bacterial strains.

Bacterium	Nanomaterial support	Recognition element/detection technique	Detection limit/working range	Reference
Escherichia coli O157:H7	MNPs	Thiolated ssDNA immobilized on quartz crystal microbalance	2.67×10^2 CFU/mL; 2.67×10^2–2.67×10^6 CFU/mL	[16]
	GNPs	*eae*A gene-specific thiolated probe conjugated to piezoelectric biosensor	1.2×10^2 CFU/mL; 10^2–10^6 CFU/mL	[17]
	GNPs	Two ABs coupled with GNPs–SPCE; DIS-amperometry	6 CFU/strip in buffer and 50 CFU/strip in milk; 10^2–10^7 CFU/mL	[18]
	PNPs	AB immobilized on PNPs–SPCE; cyclic voltammetry	—	[19]
E. coli	MNPs	Incubation of target with fluorescein-labeled concanavalin A; epifluorescent microscopy	10^4 cells/mL	[20]
	SNPs	Rabbit IgG antibody conjugated with SNPs; SPR band shift using UV–VIS spectroscopy	5–10^9 cells/mL	[21]
	Cu@GNPs	AB–Cu@GNPs; anodic stripping voltammetry	30 CFU/mL	[22]
	GNPs@CNTs	RNA-coated GNPs on CNTs; UV–VIS spectroscopy	—	[23]
Salmonella	GNPs	MAB–polystyrene coupled with PAB–GNPs; anodic stripping voltammetry	98.9 CFU/mL; 1.3×10^2–2.6×10^3 CFU/mL	[24]
	GNPs	MAB–GNPs conjugated to GCE; electrochemical impedance spectroscopy	1×10^2 CFU/mL; 1×10^2– 1×10^5 CFU/mL (pork sample)	[25]
	MNPs	AB–MNPs and AB–TiNPs; UV–VIS spectroscopy	100 CFU/mL (milk sample)	[26]
	CNTs	MAB–CNTs conjugated to GCE; electrochemical impedance spectroscopy	1.6×10^4 CFU/mL	[27]
	QDs	AB–MBs coupled with AB–biotin and streptavidin–QDs; fluorescence spectroscopy	10^3 CFU/mL; 10^3–10^7 CFU/mL (chicken carcass water)	[28]
	SNC	Extent of SNC's bending proportional to bacterial count	25 cells/mL	[29]
Listeria monocytogenes	MNPs	AB–SPIONs; magnetic flux measurement by high-transition temperature SQUID	5.6×10^6 cells/20 μL and 230 cells/1 nL	[30]
Mycobacterium avium	MNPs	AB–protein G–SPIONs at optimum SPIONs concentration of 2 μg Fe/μL; SQUID	15.5 CFU/mL; 15.5–775 CFU/mL	[31]
	GNPs	MAB–DSNB–sulfur–GNPs; SERS-based sandwich immunoassay	100 ng/mL in buffer and 200 ng/mL in pasteurized whole milk	[32]
Pseudomonas aeruginosa	GNRs	AB–GNRs by carbodiimide chemistry; NIR light-mediated staining of live/dead cells	75% decrease in cell viability	[33]
Vibrio parahaemolyticus	GNPs	Agarose–GNPs on SPCE; amperometry	7.4×10^4 CFU/mL; 10^5–10^9 CFU/mL	[35]
E. coli O157:H7, *Salmonella typhimurium* and *Bacillus cereus*	SiNPs	AB–SiNPs; plate-counting and fluorescence methods	1–400 cells (plate-counting method) single cell (fluorescence method) (ground beef sample)	[36]
Twelve different bacteria*	GNPs	Poly(para-phenylene ethynylene)–GNPs; fluorescence spectroscopy	1×10^9 CFU/mL	[37]
Eight different bacteria*	MNPs	Amine-functionalized MNPs; plate-counting method	88.8–99.1% bacteria capture (water, grape juice, green tea, and urine)	[38]

AB = antibody; CFU = colony forming units; CNTs = carbon nanotubes; Cu = copper; DIS = differential impedance spectroscopy; DSNB = 5,5′-dithiobis(succinimidyl-2-nitrobenzoate); GCE = glass carbon electrode; GNPs = gold nanoparticles; GNRs = gold nanorods; Ig = immunoglobulin; MAB = monoclonal antibody; MBs = magnetic beads; MNPs = magnetic nanoparticles; NIR = near infrared; PAB = polyclonal antibody; PNPs = peptide nanotubes; QDs = quantum dots; RNA = ribonucleic acid; SERS = surface-enhanced Raman scattering; SiNPs = silica nanoparticles; SNC = silicon-nitride cantilever; SNPs = silver nanoparticles; SPCE = screen-printed carbon electrode; SPIONs = superparamagnetic iron oxide nanoparticles; SPR = surface plasmon resonance; SQUID = superconducting quantum interference device; ssDNA = single-stranded DNA; TiNPs = titanium nanoparticles; UV–VIS = ultraviolet–visible.

* The names of bacteria are provided in the text.

with *Salmonella* spp. could be directly measured by electrochemical impedance spectroscopy with a detection limit of 1×10^2 CFU/mL, with the linear relationship between change in capacitance and logarithm of concentration being obtained in the range of 1×10^2–1×10^5 CFU/mL. Using MNPs and optical nanocrystal probes, Joo et al [29] developed a facile and sensitive method for detection of *Salmonella* in milk. The bacteria in milk were captured by antibody-conjugated MNPs, followed by separating the bacteria-adsorbed probe using an external magnetic field, exposing it again to antibody-immobilized TiO_2 nanocrystals for absorption of UV light, and then magnetically separating the MNPs–*Salmonella*–TiO_2 complexes from solution for analysis of unbound TiO_2 nanocrystals with an UV–visible spectrometer. A detection limit of 100 CFU/mL was obtained for *Salmonella* in milk [29]. In an attempt to improve the performance of electrochemical biosensor by CNTs, Jain et al [30] immobilized CNTs-functionalized monoclonal antibodies onto a glassy carbon electrode for *S. typhimurium* detection using electrochemical impedance spectroscopy as a function of change in charge transfer resistance and impedance. A detection limit of 1.6×10^4 CFU/mL was obtained with the linear response being 10^{-1} to 10^{-6} (serial dilution values of overnight bacterial culture) [30].

The use of QDs as fluorescent labels is emerging as a novel and promising class of fluorescent biosensors. For detection of *S. typhimurium* in chicken carcass wash water, Yang and Li [31] separated the bacteria from wash water using anti-*Salmonella*-antibody-coated magnetic beads and allowed them to react with secondary biotin-labeled anti-*Salmonella* antibody to facilitate reaction of biotin with streptavidin-coated QDs and measure fluorescence intensity. The linear response between logarithm of bacterial cell number and fluorescence intensity was in the range of 10^3–10^7 CFU/mL with the detection limit obtained being 10^3 CFU/mL [31]. Earlier to the aforementioned sensors for *Salmonella*, Weeks et al [32] developed a silicon nitride cantilever for detection of *Salmonella enterica* cells as low as 25 by monitoring the cantilever's surface bending, which was directly proportional to the amount of bacteria bound on cantilever.

2.3. *Listeria monocytogenes*

L. monocytogenes is the Gram-positive bacterium responsible for the infectious disease listeriosis. It is the most virulent microorganism and the third leading cause of death among foodborne bacterial pathogens. For detection of *L. monocytogenes*, Grossman et al [33] developed an interesting principle based on monitoring the binding rate between antibody-linked MNPs and bacteria using a high-transition temperature superconducting quantum interference device (SQUID). Superparamagnetic nanoparticles with a size of 50 nm coated with antibody were added to the *L. monocytogenes* sample, followed by applying pulsed magnetic field to align the magnetic dipole moments. While free nanoparticles quickly randomize by Brownian rotation, the nanoparticles bound to *L. monocytogenes* could undergo Neel relaxation and gradually dissipate magnetic flux for measurement by SQUID. A detection limit of 5.6×10^6 and 230 *L. monocytogenes* cells were obtained in a sample of 20 μL and 1 nL, respectively [33]. A similar magnetic relaxation technique was also used for detection of mycobacterial species, which will be described in the following section.

2.4. *Mycobacterium avium*

Mycobacterium avium subspecies *paratuberculosis* (MAP) is the causative agent of Johne's disease in cattle and the existing major obstacle in controlling the spread of this disease lies in the inability to rapidly detect this microorganism in small concentrations. Recent advances in developing nanosensors provide attractive solutions for fast, sensitive, and high-throughput analysis [6,34,35]. Kaittanis et al [34] developed a one-step nanoparticle-mediated bacterial detection method in milk and blood by exploiting the magnetic relaxation property of superparamagnetic iron oxide nanoparticles (SPIONs). The principle underlying the detection mechanism by magnetic nanosensors is based on their ability to switch between dispersed and clustered state during target interaction, resulting in a concomitant change in spin–spin relaxation time. For detection of MAP, the SPIONs were conjugated with anti-MAP antibodies through protein G and the nanosensors were shown to respond in a dose-dependent manner upon addition of MAP, with the method working best at a nanoparticle concentration of 2 μg Fe/μL. Accordingly, the MAP-spiked whole milk conjugated with 2 μg Fe/μL MAP nanosensor showed a change in T2, which was indirectly proportional to the MAP concentration, with the reliable quantitation being attained in the range of 15.5–775 CFUs after a 30-minute incubation at room temperature [34]. However, at 37°C, the detection and quantitation of MAP could be achieved with high sensitivity in 2% milk. One more advantage is that a 30-minute incubation at 37°C did not affect the detection sensitivity in the presence of some other bacteria such as *E. coli*, *S. aureus*, *Pseudomonas aeruginosa*, *Enterococcus faecalis*, *Proteus vulgaris*, and *Serratia marcescens*, but increasing the incubation time to 45 minutes increased the detection limit from 15.5 CFUs to 38.8 CFUs. Furthermore, this single-step assay could also determine whether the blood samples from an individual were MAP positive or negative [34]. In another study, Yakes et al [35] developed a sandwich immunoassay for rapid, low-level detection of MAP based on surface-enhanced Raman scattering (SERS) with two key components through immobilization of monoclonal antibody 13E1 for targeting a surface protein MAP2121c on microorganism and designing extrinsic Raman labels with 60-nm GNPs for selective binding of captured proteins to produce large SERS signals. The application of Raman spectroscopy in the analysis of food and pharmaceutical nanomaterials was recently reviewed by Li and Church [36]. The development of Raman label was based on spontaneous adsorption of sulfur compounds onto GNPs, followed by 5,5′-dithiobis(succinimidyl-2-nitrobenzoate) (DSNB) adlayer formation on the surface of nanoparticle, which can tether antibodies, resulting in the formation of a biospecific label [35]. The detection was based on quantitation of intensity of strong $\nu_s(NO_2)$ of the DSNB-derived monolayer. This Raman label-incorporated SERS-based immunoassay was able to detect MAP within 24 hours at a level as low as 100 ng/mL in PBS and 200 ng/mL in pasteurized whole milk through integration of 13E1

monoclonal antibody as recognition element in SERS. A high reproducibility shown by this method could be attributed to the formation of uniform nanoparticles and preparation of optimized Raman labels [35].

2.5. *Pseudomonas aeruginosa*

The common Gram-negative *P. aeruginosa* bacterium is known for its ability to cause inflammation and sepsis. Most importantly, its colonization in certain organs such as the lung, urinary tract, and kidney can be lethal. It is also responsible for cross infections in hospital and clinical equipment such as catheters. The ability of gold nanorods to selectively destroy *P. aeruginosa* was explored by Norman et al [37]. The amine-terminated gold nanorods were covalently linked with carboxylic acids of anti-*P. aeruginosa* primary antibodies in the presence of 1-ethyl-3-(3-dimethylaminopropyl)carbodiimide through carbodiimide chemistry. Then, the suspension containing antibody–nanorod conjugate and bacteria was irradiated with near-infrared (NIR) light (785 nm; 50 mW) for 10 minutes, followed by staining with live (green)/dead (red) stains and counting of live versus dead cells. Compared with the 80% cell viability shown for both NIR-exposed cells without nanorods and cells with nanorods unexposed to NIR, the exposure of nanorod-coated *P. aeruginosa* cells to NIR radiation exhibited a 75% decrease in cell viability [37].

2.6. *Vibrio parahaemolyticus*

Food poisoning associated with *V. parahaemolyticus* is common among people consuming raw and undercooked shellfish in diet [2,3]. Taking advantage of the recent progress in analytical nanotechnology, Zhao et al [38] have developed a disposable enzyme immunosensor based on a screen-printed electrode coated with agarose-doped GNPs for detection of *V. parahaemolyticus*. The GNPs provided a short conduction pathway for efficient and direct electron transfer because of drastic reduction in the distance between the active site and electrode. Upon incubation of *V. parahaemolyticus*-incorporated sensor for 30 minutes at 25°C, the bacterium formed an immunocomplex with horseradish peroxidase (HRP) and anti-*V. parahaemolyticus* on the sensor surface and the amperometric detection was based on reduction in cathodic peak current caused by inhibition of enzyme activity, which was responsible for oxidation of thionine by H_2O_2 [38]. The authors have also demonstrated high selectivity in the presence of some other common food pathogens such as *E. coli* O157:H7, *Salmonella pullorum,* and *S. aureus*, but failed to validate the method in real food samples.

2.7. *Multiplex detection of bacterial pathogens*

The multiplexing capability of a method for simultaneous detection of multiple bacterial pathogens is particularly attractive. Taking multiple detection of *E. coli* O157:H7, *S. typhimurium,* and *B. cereus* as an example, Zhao et al [39] used antibody-conjugated dye-doped silica nanoparticles for incubation of bacteria, followed by removing any unbound nanoparticles through centrifugation, and detecting bacteria by the plate-counting method. This method could not only be completed within 20 minutes, but also facilitated accurate quantitation of *E. coli* O157:H7 in spiked ground beef samples with the detection limit being 1–400 cells. In addition, some other bacterial species such as *S. typhimurium* and *B. cereus* could be quantified, indicating the wide application of this method for detecting both Gram-negative and Gram-positive microorganisms [39]. Although both gold-standard plate-counting and fluorescent-nanoparticle methods provided similar results, the latter was faster, compared with plate counting, which required 16 hours. Furthermore, this method facilitated high-throughput capability with detection even down to single bacterial cell, and thus, its application could be envisaged for ultrasensitive detection of disease markers and infectious agents. In a similar study, the GNPs were conjugated with π-conjugated polymer poly(para-phenylene ethynylene) for positive identification of 12 different bacterial strains within a few minutes [40]. Upon nanoparticle–bacteria interaction, the bound fluorescent polymer was released from GNP quencher emitting fluorescence. Moreover, the negatively charged bacterial cell membrane could also displace the polymer from GNPs thereby further enhancing the fluorescence emission. Three different nanoparticle preparations were prepared by the authors and distinct fluorescence could be observed for each bacterium including *Amycolatopsis azurea*, *Amycolatopsis orientalis*, *Bacillus licheniformis*, *Bacillus subtilis*, some *E. coli* strains (BL21DE3, DH5α, and XL1-Blue), *Lactobacillus lactis*, *Lactobacillus plantarum*, *Pseudomonas putida*, *Streptomyces coelicolor,* and *Streptomyces griseus* [40]. For quantitation, a signature plot was constructed for pattern recognition through linear discriminant analysis. The major advantage of this method is its affordability and robust bacterial identification capability without the need for heat-labile antibody-conjugated probes. However, its detection limit is high (1×10^9 CFU/mL). The sensitivity of this method can be improved by further optimization of conditions and employing some other polymer conjugates [40]. More recently, Huang et al [41] prepared amine-functionalized MNPs (AF-MNPs) for rapid and high efficiency (88.5–99.1%) capture of both Gram-negative and Gram-positive bacteria from water, food matrices, and urine. A high-affinity adsorption toward eight bacteria including *Sarcina lutea*, *S. aureus*, *E. coli*, *B. cereus*, *B. subtilis, Salmonella*, *P. vulgaris,* and *P. aeruginosa* was shown to occur based on the electrostatic interaction between positively charged AF-MNPs and negatively charged sites of the bacterial surface. The amount of AF-MNPs, pH of phosphate buffer, and ionic strength were shown to be crucial in mediating fast and effective interaction [41]. The advantages of this method are short incubation time and high capture efficiency requiring no further modification of biomolecules on AF-MNPs. However, the major pitfall is less specificity/selectivity when compared with some other methods using antibody conjugates.

3. Nanomaterial-based sensors for detection of bacterial and food toxins

Table 2 shows a collection of some reported studies on nanomaterial-based sensors used for detection of bacterial and food toxins.

Table 2 – Some reported nanomaterial-based sensors for detection of different bacterial and food toxins.

Toxin	Nanomaterial support	Recognition element/detection technique	Detection limit/working range	Reference
Cholera	CNTs	MAB–PEDT–MWCNT on GCE and AB–ganglioside@liposome; voltammetry	10^{-16} g/mL; 10^{-14}–10^{-7} g/mL	[39]
	GNPs	GNPs–ganglioside@lipid bilayer support; fluorescence method	10–100pM; 10pM–100nM	[40]
	GNPs	Thiolated lactose–GNPs; UV–VIS spectroscopy	3 μg/mL	[41]
Staphylococcal enterotoxin	CNTs	AB–AB(HRP)–CNTs; fluorescence method	0.1 ng/mL; 0.1–100 ng/mL	[42]
	GNPs	AB–GNPs on polycarbonate surface; ELISA coupled with ECL detection	0.01 ng/mL	[43]
Shiga toxin	GNPs	Glyconanoparticles–GNPs; SPR competition assay	—	[44]
	GPNPs	Chromatic sensor; UV–VIS spectroscopy	1200 U/μL; 1200–7200 U/μL	[45]
Ricin	GNPs	Thiolated β-lactosylceramide ligand–GNPs; UV–VIS spectroscopy	<3.3 μg/mL in 10 min, 1.7 μg/mL in 30 min	[46]
	GNPs	GM1 receptor–biotin–streptavidin–GNPs; UV–VIS spectroscopy	0.83–5.83nM	[47]
Brevetoxins	GNPs	BTX(BSA)–GNPs–PAADs and HRP–AB; competitive-type electrochemical immunosensor	0.01 ng/mL; 0.03–8 ng/mL	[48]
Cholera, Shiga toxin, ricin, and staphylococcal enterotoxin B	QDs	AB–CdSe–ZnS@QDs; fluoroimmunoassay	—	[49]
Escherichia coli O157:H7, *Salmonella enterica*, and staphylococcal enterotoxin B	MNPs	DNA–AB–MNPs; fluorescence method	2.4×10^3 CFU/mL (*E. coli*), 1.9×10^4 CFU/mL (*S. enterica*), 0.11 ng/mL (staphylococcal enterotoxin B) (in buffer and milk samples)	[50]

AB = antibody; BSA = bovine serum albumin; BTX = brevetoxins; CFU = colony forming units; CNTs = carbon nanotubes; ECL = enhanced chemiluminescence; ELISA = enzyme-linked immunosorbent assay; GCE = glass carbon electrode; GM1 = ganglioside-monosialic acid 1; GNPs = gold nanoparticles; GPNPs = glycopolydiacetylene nanoparticles; HRP = horseradish peroxidase; MAB = monoclonal antibody; MNPs = magnetic nanoparticles; MWCNT = multiwalled carbon nanotubes; PAADs = polyamidoamine dendrimers; PEDT = poly(3,4-ethylenedioxythiophene); QDs = quantum dots; SPR = surface plasmon resonance; UV–VIS = ultraviolet–visible.

3.1. *Cholera toxin*

Cholera toxin (CT), a protein complex secreted by the bacterium *Vibrio cholera*, is responsible for the watery diarrhea during cholera infection. Structurally, it is an oligomeric complex denoted by AB_5 and composed of six protein subunits (a single copy of the A subunit and five copies of the B subunit) [6,9]. Recent developments in nanoparticle application in sensor devices enabled Viswanathan et al [42] to develop a sensitive method for detection of CT using an electrochemical immunosensor with liposomic magnification by linking an anti-CT-B subunit monoclonal antibody with poly(3,4-ethylenedioxythiophene) coated on Nafion-supported multi-walled CNT film in a glassy carbon electrode. The detection was based on sandwich-type assay involving electronic transducers in which the toxin is first bound to the anti-CT antibody followed by conjugation with ganglioside-functionalized liposome. The potassium ferrocyanide molecules released from liposomes bound onto electrode were measured by adsorptive square-wave stripping voltammetry. The detection limit and linear working range of CT were 10^{-16} g/mL and 10^{-14}–10^{-7} g/mL, respectively [39]. In another study, GNPs were tethered on supported ganglioside-containing lipid bilayer for detection of CT [43]. A 100-fold improvement in sensitivity could be achieved by this method when compared with other typical fluorescent immunoassays (5nM), with the detection limit and linear dynamic range being 10–100pM and 10pM–100nM, respectively [43]. In a colorimetric bioassay developed by Schofield et al [44], a thiolated-lactose derivative self-assembled on GNPs (16 nm) aggregated upon binding to the CT-B subunit, and the detection principle was based on a color change from red to purple. The limit of detection was estimated to be 3 μg/mL.

3.2. *Staphylococcal enterotoxin*

Staphylococcal enterotoxins (SEs), an important group of 21 heat-stable toxins produced by *S. aureus*, are associated with foodborne diseases resulting from consumption of contaminated foods [9,45,46]. The food poisoning due to SEs causes anorexia, nausea, vomiting, and diarrhea even at low levels (20–100 ng/person) of exposure [9]. In addition, SEs have been associated with the occurrence of diseases such as atopic eczema, rheumatoid arthritis, and toxic shock syndrome [45,46]. Although the existing detection methods such as ELISA and some other immunological assays provide speed and high throughput, they do not provide sufficient sensitivity in all applications. To overcome this drawback, Yang et al [45] developed an optical immunosensor using CNTs for detection of SEs through binding with anti-SE primary antibody immobilized on CNT followed by binding of HRP-labeled secondary antibody and detection of HRP fluorescence. This sandwich immunosensor-based assay could provide a signal six to eight times larger than that of the standard-type immunosensor with the detection limit and linear dynamic range being 0.1 ng/mL and 0.1–100 ng/mL, respectively. However, the application of this assay to real food samples such as soy milk, apple juice, meat, and baby food required an additional sample purification step by carboxymethyl cellulose chromatography [45]. In a later study, the same research group evaluated the GNPs-based enhanced chemiluminescence (ECL) immunosensor for detection of SEs in food [46]. The anti-SE primary antibody was immobilized onto a GNP surface through physical adsorption, and the antibody–GNPs conjugate was immobilized onto a polycarbonate surface. The sandwich-type ELISA developed was based on detection using secondary antibody (HRP-conjugated antirabbit IgG) for ECL detection [46]. The limit of detection (0.01 ng/mL) of this method was found to be 10 times more sensitive than the traditional ELISA method as well as the CNT-based immunosensor assay as described earlier [45,46]. More importantly, GNPs are not only less toxic than CNTs, but also do not require shortening and acid functionalization, thereby making the preparation of GNPs-based immunosensor much easier.

3.3. *Shiga toxin*

Shiga-like toxins, belonging to the same family as the CT, are produced by *E. coli*, especially the foodborne pathogen *E. coli* 0157:H7. Interestingly, the B subunit of Shiga-like toxin produced by *E. coli* 0157:H7 specifically recognizes the globotriose (P^k) blood group antigen, which contains the trisaccharide αGal(1→4)βGal(1→4)βGlc, and each of five B subunits has three available binding sites for P^k [6,47]. By exploiting this phenomenon, Chien et al [47] developed an SPR competition assay using glyconanoparticles obtained by self-assembling two derivatives of P^k onto GNPs of different sizes (4 nm, 13 nm, and 20 nm). The longer chain length was shown to enhance binding affinity of the P^k moiety, resulting in a greater flexibility of P^k ligand to bind onto more sites on the toxin surface. Likewise, a greater binding affinity was shown by the P^k–gold derivatives prepared with GNPs of larger diameter, which was attributed to the lower curvature of GNPs. Based on these outcomes, a chip-based assay was developed through the incorporation of glyconanoparticles [47]. In another study, Nagy et al [48] further developed a chromatic sensor with Gal-α1,4-Gal glycopolydiacetylene as nanoparticle for selective detection of Shiga toxin-producing *E. coli* O157:H7. The well plates containing Shiga toxin-producing *E. coli* O157:H7 could change the color from purple to brown within 5 minutes, whereas the non-Shiga toxin producing *E. coli* solution remained purple upon addition of glycopolydiacetylene nanoparticles. This method was shown to be highly selective, rapid, and sensitive, with the limit of detection and linear dynamic range being 1200 U/μL and 1200–7200 U/μL, respectively [48].

3.4. *Ricin*

Owing to its illegal use, ricin (*Ricinus communis*), a highly toxic lectin, is now considered a bioterrorism threat. The mechanism of toxicity arises from binding of its two carbohydrate active sites to β-D-galactopyranose or β-D-N-acetylgalactosamine residues on the surface of the host cell [6,49]. Based on this toxicity mechanism, Uzawa et al [49] developed a facile and sensitive colorimetric assay for ricin using GNPs functionalized with a thiolated β-lactosylceramide ligand. Upon addition of ricin (RCA_{60}) or its surrogate agglutinin RCA_{120} to glycol nanoparticles, a visual change of color from red to purple occurred and this color change was not observed in the

presence of several other plant lectins including those from jack bean, soybean, peanut, clary sage, osage orange, and Amur maackia trees, as well as in the presence of noncarbohydrate-binding proteins [bovine serum albumin (BSA) and γ-globulin]. This bioassay could detect ricin at concentrations less than 3.3 μg/mL in 10 minutes or 1.7 μg/mL in 30 minutes. In another study, Taylor et al [50] combined the sensitivity of SPR and facile construction of microfluidic devices from polydimethylsiloxane by tethering ganglioside-monosialic acid 1 receptor-containing lipid vesicles on gold nanoglassified surface through anchoring the vesicle's biotin moieties to the surface-interacting streptavidin molecules. Although the detection limit (0.83–5.83nM) obtained by this method was not as sensitive as the other methods, further improvements in both device designing and signal amplification could significantly enhance its sensitivity and multiplexing capability.

3.5. *Brevetoxins*

Brevetoxins (BTXs) are cyclic polyether ladder neurotoxins produced by the dinoflagellate *Karenia brevis* (marine microorganism), which can bind to voltage-sensitive sodium channels in cell membranes, leading to neurotoxic shellfish poisoning characterized by paresthesia, reversal of hot–cold temperature sensation, muscle pain, vertigo, loss of coordination, abdominal pain, nausea, diarrhea, headache, slow heart rate, dilated pupils, and respiratory irritation [9]. For rapid screening of BTX-B in food samples, Tang et al [51] developed a sensitive electrochemical immunosensor by immobilizing BTX-B–BSA conjugate on GNPs-decorated amine-terminated polyamidoamine dendrimers (GNP–PAADs). On the basis of the competitive-type immunoassay format with the HRP-labeled anti-BTX antibodies as sensor label, a low detection limit of 0.01 ng/mL was obtained with a wide working linear range of 0.03–8 ng/mL BTX-B. The incorporation of GNPs and three-dimensional PAADs could substantially enhance the conductivity of PAADs and surface coverage of biomolecules on the electrode, respectively [51].

3.6. *Multiplex detection of bacterial and food toxins*

In an attempt to simultaneously detect multiple toxins, multiplexed fluoroimmunoassays were developed by conjugating highly luminescent semiconductor nanocrystals (CdSe–ZnS core-shell QDs) and antibodies for analyzing CT, ricin, Shiga-like toxin, and SE B [52]. This sandwich immunoassay could quantify all the four toxins in a single sample by a high-throughput format. Although this method overcomes the multiple isolation and incubation steps as required in any typical immunoassay, the cross-reactivity was shown to be problematic. However, it was suggested that through the careful optimization of assay conditions and selection of the antibody reagent, the problem associated with cross-reactivity could be solved for attaining reliability and robustness. In a previous study, Branen et al [53] developed an enzyme bionanotransduction assay for simultaneous detection of *E. coli* O157:H7, *S. enterica* serovar *typhimurium*, and SE B in both buffer and milk with the limit of detection obtained being 2.4×10^3 CFU/mL, 1.9×10^4 CFU/mL, and 0.11 ng/mL, respectively. This fluorescence-based assay could quantify all the three toxins through adsorption onto antibody–MNPs conjugate and amplification of DNA templates bound onto the antibody.

4. Nanomaterial-based detection of pork adulteration in meat products

More recently, the GNPs have been successfully demonstrated as a potential sensor for detection of pork adulteration in beef and chicken meatball preparations [11–14]. On the basis of an interesting noncross-linking method [54,55], Ali et al [13] developed an analytical method using 20-nm citrate-coated GNPs to determine pork adulteration in beef and chicken meatball preparations. The basic principle for analysis involved measurement of change in color of GNPs from red to purple grey in vials containing swine DNA, with red remaining unchanged in nonpork samples (chicken or beef). More elaborately, the GNPs were well dispersed in deionized water without incubation and also dispersed in 3mM PBS after a 3-minute incubation of GNPs with 3nM single-stranded DNA probe at 50°C. In contrast, the GNPs aggregated in 3mM PBS without incubation and also aggregated in 3mM PBS after a 3-minute incubation of GNPs with 3nM double-stranded DNA probe at 25°C, resulting in a change in color of GNPs from red to purple grey (Fig. 1A and 1B) [13]. In general, the negative coatings of citrate ions on the GNP surface electrostatically repel each other providing good dispersion of GNPs in deionized water. Likewise, the single-stranded DNA adsorbed on GNPs by van der Waals interactions provides more phosphate-negative charges on GNP surfaces further stabilizing the GNPs. However, the aggregation of GNPs in PBS can be attributed to the reduction of repulsive negative charges between individual GNPs. In addition, unlike single-stranded DNA, the double-stranded DNA could not protect the GNPs from salt-induced aggregation because of the highly stable and uncoiled nature of the latter (Fig. 1B). This phenomenon could be clearly visualized in transmission electron microscopy (TEM) images and in the absorption spectra as shown in Fig. 1A [13].

Application to real samples involved mixing and annealing (50°C) of a 25-nucleotide (nt) single-stranded DNA probe with 95°C-denatured DNA from different meatballs differentiated well between perfectly matched swine *cytb* gene and mismatched hybridization (13- and 14-nt mismatching with bovine and chicken *cytb* genes, respectively) [13]. Consequently, the vials containing nonpork DNA did not engulf probes due to mismatches and single-stranded DNA adsorbed on GNPs protected GNPs from salt-induced aggregation, whereas the probes were completely consumed by perfect hybridization in vials containing pork in pure and mixed forms, accompanied by a color change of GNPs from red to grey due to aggregation, leading to an eventual red shift in SPR peak from 525 nm to 575 nm and appearance of an additional peak at 610 nm (Fig. 1C) [13]. Similarly, the original pinkish red color that appeared in 1% pork was considerably reduced in 3–5% pork containing vials resulting in a wavelength shift from 525 to 535 nm and appearance of a stronger absorption between 550 and 650 nm due to partial aggregation. Whereas, a complete aggregation occurred in 10% and 15% pork

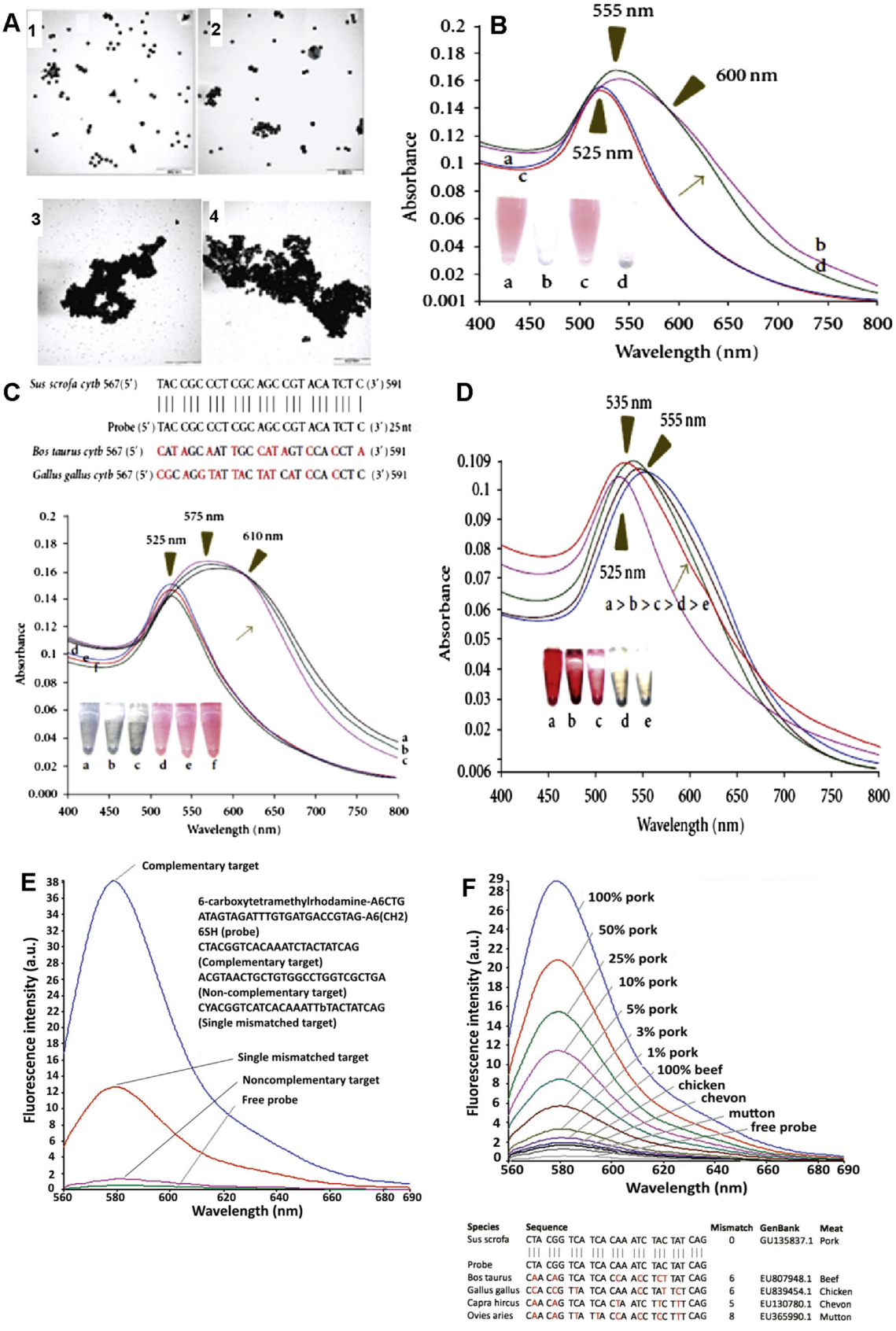

Fig. 1 – Identification and quantitation of pork adulteration in meatball formulations. (A) TEM images of GNPs before and after salt-induced aggregation. Panels A1 and A2 denote GNPs dispersed in deionized water and in 3mM PBS after a 3-minute incubation with 3nM single-stranded DNA, respectively. Panels A3 and A4 indicate GNPs aggregated in 3mM PBS and in 3mM PBS after a 3-minute incubation with 3nM double-stranded DNA probe. (B) Absorption spectra of aggregated

containing vials as evident from the change in color from pinkish red into purple grey (Fig. 1D) [13]. In another study, a species-specific nanobiosensor was fabricated by integrating a 27-nt *AluI* fragment with 3-nm citrate–tannate-coated GNPs [12]. Structurally, the nanobiosensor was composed of a single-stranded DNA covalently linked to 3-nm GNPs via sulfur–gold bond at one end and a fluorescent dye at the other end. The higher the fluorescence emission, the greater the degree of target DNA binding, with the baseline and maximum fluorescence being observed in the absence of any target DNA and by saturating the probe with target DNA, respectively. The underlying mechanism of this method involves three oligonucleotide probes flanked by a hexyl-A spacer at both sides, while the alkane thiol cap at one end and fluorophore at the other end are shown to self-organize in a constrained arch-like structure [12]. In the absence of any complementary target, the fluorophore is quenched by GNPs. However, upon target binding, the structure of probe is transformed into a rod-like conformation emitting fluorescence due to separation of fluorescence dye from the nanoparticle. In addition, the distinct change in fluorescence intensity was shown to occur among noncomplementary, complementary, and single mismatched targets as compared with that for free probe, demonstrating the high specificity of this method (Fig. 1E). Moreover, this swine-specific biosensor could detect 100% pork and 1–50% pork in ready-to-eat meatballs prepared from pork–beef mixtures with high sensitivity and specificity. Commercial meatballs made from beef, chicken, mutton, and chevon also showed significant difference in fluorescence intensity when compared with free probe (Fig. 1F) [12].

Differently sized GNPs have been reported to affect the limit of detection of swine DNA in pork-adulterated meatball preparations. In three different studies, the GNPs of different sizes such as 40 nm, 20 nm, and 3 nm were shown to detect pork adulteration with different sensitivity yielding a limit of detection value of 6 μg/mL, 4 μg/mL, and 0.23 μg/mL of swine DNA in 20%, 10%, and 1% pork-containing meatballs, respectively [11–13]. The limit of detection can be further reduced by increasing the amount of DNA mixtures to ensure sufficient targets for the probe, which should not be a problem especially in food analysis where the sample scarcity is not a major concern. Furthermore, it has been demonstrated that the 20-nm GNPs could produce a more pronounced change in color and absorption spectra compared with their 40-nm counterparts [11–13]. This method provides a simple, sensitive, and selective detection at an affordable cost using the commonly available UV–visible spectrophotometer. In addition, compared with conventional PCR methods, this method is rapid (<10 minutes) and highly sensitive, which requires only shorter DNA targets and possesses the ability to analyze highly degraded samples. However, the major disadvantage of this nanobiosensor assay is that it fails to provide quantitative information of the target DNA [11–13].

Most of the available DNA sequence-detecting assays rely on PCR followed by electrophoretic visualization of PCR products. However, the PCR-based assays require high reagent and instrument costs as well as subsequent analysis by restriction fragment length polymorphism for authentication of specific sequences in PCR products [11–14]. In addition, the complicated synthetic chemistry required to modify the DNA, substrates, or nanoparticles and for hybridization on surfaces could impose serious steric constraints, making the analysis of PCR products both expensive and time consuming because of low and inefficient binding of probe and target [11,14]. For many years, the distinct optical property (SPR) exhibited by colloidal GNPs has been studied for sensing specific oligonucleotide sequences in several fields including biodiagnostics, genetics, and food analysis [11–14]. Nevertheless, all these studies based on cross-linking mechanism require surface

and nonaggregated GNPs with blue and pink curves representing GNPs dispersed in deionized water and aggregated in 3mM PBS, respectively, whereas red and green curves denote GNPs dispersed in 3mM PBS after a 3-minute incubation with 3nM single-stranded DNA and aggregated in 3mM PBS after a 3-minute incubation with 3nM double-stranded DNA. (C) Identification of swine DNA in mixed meatball with comparison of probe sequences and mismatch bases shown in red color as well as vials (a–f) indicating GNPs color in genomic DNA extracted from meatballs prepared from (a) pure pork, (b) 1:1 (w/w) mixtures of pork–beef, (c) pork–chicken, (d) chicken–beef, (e) pure beef, and (f) pure chicken and their corresponding absorption spectra. (D) Determination of limit of detection for pork in ready-to-eat beef meatballs with vials (a–e) showing the GNPs color in (a) 1%, (b) 3%, (c) 5%, (d) 10%, and (e) 15% pork DNA extracted from processed pork–beef meatballs and their corresponding absorption spectra. (E) The probe and oligonucleotide sequences (5′→3′) used and the corresponding fluorescence detection of specific DNA sequences and single nucleotide mismatches by swine-specific nanobiosensor probes at excitation wavelength of 545 nm. (F) Fluorescence spectra at excitation wavelength of 545 nm depicting pork detection in ready-to-eat port–beef mixed and commercial meatballs as well as the corresponding comparison of nucleotide sequences of different species with swine oligo probe shown along with mismatched bases in red. *Note.* Fig. 1A and 1B: Reference 11 are from "Use of nanomaterials in the detection of food contaminants," by S.K. Sonawane, S.S. Arya, J.G. LeBlanc, and N. Jha, 2014, *Eur J Nutr Food Saf* 4, p. 301–17. © 2011 IOP Publishing Ltd. Adapted with permission. Fig. 1C and 1D: Reference 13 are from "Nanoparticle sensor for label free detection of swine DNA in mixed biological samples," by M.E. Ali, U. Hashim, S. Mustafa, Y.B. Man, M.H. Yusop, M.F. Bari, Kh.N. Islam, and M.F. Hasan, 2011, *Nanotechnology 22*, 195503. © 2012 M.E. Ali et al., an open access journal distributed under Creative Commons Attribution License and published by Hindawi Publishing Corporation. Adapted with permission. Fig. 1E and 1F: Reference 12 are from "Listeriolysin O: a key protein of *Listeria monocytogenes* with multiple functions," by S. Kayal and A. Charbit, 2006, *FEMS Microbiol Rev* 9, p. 76–85. © 2012 Taylor & Francis. Adapted with permission. GNPs = gold nanoparticles; PBS = phosphate-buffered saline; TEM = transmission electron microscopy.

modification of GNPs to immobilize two DNA probes, followed by further cross-linking using a complementary target to induce aggregation. This limitation could be overcome through detection of nucleotide sequences using a noncross-linking method pioneered by Sato et al [54] as well as by Li and Rothberg [55]. More importantly, the nanoparticle-based assay described above for detection of pork adulteration is based on the noncross-linking method, which does not require any modification chemistry or target hybridization. Thus, it may be envisaged that the analytical method based on noncross-linking could be adopted to solve problems in a wide variety of biological scenarios in the future.

Overall, the much needed effective detection of pathogens in clinical, food, and environmental samples can be facilitated by nanomaterial-based sensors. Although several new detection methods such as radiometric (BACTEC) and the Micro-ID procedures have considerably reduced the incubation time, the nanomaterial-based sensors can detect pathogens and toxins at very low concentrations as they can react and produce a strong signal in a very short incubation time. However, there is still a need for critical evaluation of the toxicity of nanomaterials used in analytical methods as pointed out in several articles [56–62]. In addition, based on the conclusion drawn out of a 10-year BioWatch project (2003–2013) conducted by the U.S. Department of Homeland Security, it is important to emphasize that the detection of pathogens and toxins under a controlled laboratory environment can be quite different compared with the same analytical technique applied in a real-time field test [63]. For example, several factors associated with meat such as types of meat, methods of raising and handling of animals by different farmers/workers, variations among different subspecies of animals, and various degrees of endogenous microbial population in the meat can cause significant variations in sample matrix and eventual complexity in detection. Thus, the detection of foodborne pathogens and toxins by nanomaterial-based sensors should predominantly focus on validating the method in real samples as well as evaluating purification and isolation steps for absolute identification of pathogens in samples containing diverse matrix.

5. Conclusion and future perspective

This review has highlighted the promising role of nanomaterials and their potential in the field of food analysis. Nanomaterial-based sensors involve binding or reaction of biological components with target species and transforming eventually into detectable signals, thereby enabling rapid detection of food contaminants and ensuring food safety for prompt preventive action. In addition, they provide advantages of rapid, sensitive, and user-friendly detection, enabling portability for in-field application. However, several issues including interference in real-sample analysis, reproducibility, and toxicity of nanomaterials remain to be solved. Besides, as most of the studies have focused mainly on GNPs, the feasibility of several other nanomaterials such as QDs, CNTs, metal oxide/metal nanoparticles, nanowires, and nanorods still need to be evaluated in designing nanosensors for possible application in food analysis.

Conflicts of interest

There is no potential conflict of interest to declare.

REFERENCES

[1] Centers for Disease Control and Prevention. Available from: http://www.cdc.gov/features/foodborne-diseases-data/ [Last accessed 16.02.15].

[2] Valdés MG, González ACV, Calzón JAG, Díaz-García ME. Analytical nanotechnology for food analysis. Microchim Acta 2009;166:1–19.

[3] Cheng W-C, Kuo C-W, Chi T-Y, Lin L-C, Lee C-H, Feng R-L, Tsai SJ. Investigation on the trend of food-borne disease outbreaks in Taiwan (1991–2010). J Food Drug Anal 2013;21:261–7.

[4] López BP, Merkoçi A. Nanomaterials based biosensors for food analysis applications. Trends Food Sci Technol 2011;2:625–39.

[5] Leonard P, Hearty S, Brennan J, Dunne L, Quinn J, Chakraborty T, O'Kennedy R. Advances in biosensors for detection of pathogens in food and water. Enzyme Microb Technol 2003;32:3–13.

[6] Kaittanis C, Santra S, Perez JM. Emerging nanotechnology-based strategies for the identification of microbial pathogenesis. Adv Drug Deliv Rev 2010;62:408–23.

[7] Salyers AA, Whitt DD. Bacterial pathogenesis: a molecular approach. 2nd ed. Washington DC: ASM Press; 2002.

[8] Manguiat LS, Fang TJ. Evaluation of DADTM kits for the detection of food-borne pathogens in chicken- and meat-based street-vended foods. J Food Drug Anal 2013;21:198–205.

[9] Sonawane SK, Arya SS, LeBlanc JG, Jha N. Use of nanomaterials in the detection of food contaminants. Eur J Nutr Food Saf 2014;4:301–17.

[10] Kayal S, Charbit A, Listeriolysin O. a key protein of *Listeria monocytogenes* with multiple functions. FEMS Microbiol Rev 2006;9:76–85.

[11] Ali ME, Hashim U, Mustafa S, Man YB, Yusop MH, Bari MF, Islam KhN, Hasan MF. Nanoparticle sensor for label free detection of swine DNA in mixed biological samples. Nanotechnology 2011;22:195503.

[12] Ali ME, Hashim U, Mustafa S, Che Man YB, Adam T, Humayun Q. Nanobiosensor for the detection and quantification of pork adulteration in meatball formulation. J Exp Nanosci 2014;9:152–60.

[13] Ali ME, Hashim U, Mustafa S, Che Man YB, Islam KN. Gold nanoparticle sensor for the visual detection of pork adulteration in meatball formulation. J Nanomater 2012;2012:103607.

[14] Ali ME, Hashim U, Mustafa S, Che Man YB, Yusop MHM, Kashif M, Dhahi TS, Bari MF, Hakim MA, Latif MA. Nanobiosensor for detection and quantification of DNA sequences in degraded mixed meats. J Nanomater 2011;2011:781098.

[15] Fan Z, Fu PP, Yu H, Ray PC. Theranostic nanomedicine for cancer detection and treatment. J Food Drug Anal 2014;22:3–17.

[16] Jain KK. Nanotechnology in clinical laboratory diagnostics. Clin Chim Acta 2005;358:37–54.

[17] Rosi NL, Mirkin CA. Nanostructures in biodiagnostics. Chem Rev 2005;105:1547–62.

[18] Nath S, Kaittanis C, Tinkham A, Perez JM. Dextran-coated gold nanoparticles for the assessment of antimicrobial susceptibility. Anal Chem 2008;80:1033–8.

[19] Mao X, Yang L, Su X, Yi Y. A nanoparticle amplification based quartz crystal microbalance DNA sensor for detection of *Escherichia coli* O157:H7. Biosens Bioelectron 2006;21:1178–85.
[20] Chen SH, Wu VC, Chuang YC. Using oligonucleotide-functionalized Au nanoparticles to rapidly detect foodborne pathogens on a piezoelectric biosensor. J Microbiol Methods 2008;73:7–17.
[21] Lin YH, Chen SH, Chuang YC, Lu YC, Shen TY, Chang CA, Lin CS. Disposable amperometric immunosensing strips fabricated by Au nanoparticles-modified screen-printed carbon electrodes for the detection of foodborne pathogen Escherichia coli O157:H7. Biosens Bioelectron 2008;23:1832–7.
[22] Cho CE, Choi J-W, Lee M, Koo K-K. Fabrication of an electrochemical immunosensor with self-assembled peptide nanotubes. Colloids Surf A Physicochem Eng Asp 2008;313–314:95–9.
[23] El-Boubbou K, Gruden C, Huang X. Magnetic glyco-nanoparticles: a unique tool for rapid pathogen detection, decontamination, and strain differentiation. J Am Chem Soc 2007;129:13392–3.
[24] Kalele SA, Kundu AA, Gosavi SW, Deobagkar DN, Deobagkar DD, Kulkarni SK. Rapid detection of *Escherichia coli* by using antibody-conjugated silver nanoshells. Small 2006;2:335–8.
[25] Zhang X, Geng P, Liu H, Teng Y, Liu Y, Wang Q, Zhang W, Jin L, Jiang L. Development of an electrochemical immunoassay for rapid detection of *E. coli* using anodic stripping voltammetry based on Cu@Au nanoparticles as antibody labels. Biosens Bioelectron 2009;24:2155–9.
[26] Maurer EI, Comfort KK, Hussain SM, Schlager JJ, Mukhopadhyay SM. Novel platform development using an assembly of carbon nanotube, nanogold and immobilized RNA capture element towards rapid, selective sensing of bacteria. Sensors (Basel) 2012;12:8135–44.
[27] Dungchai W, Siangproh W, Chaicumpa W, Tongtawe P, Chailapakul O. *Salmonella typhi* determination using voltammetric amplification of nanoparticles: a highly sensitive strategy for metalloimmunoassay based on a copper-enhanced gold label. Talanta 2008;77:727–32.
[28] Yang GJ, Huang JL, Meng WJ, Shen M, Jiao XA. A reusable capacitive immunosensor for detection of *Salmonella* spp. based on grafted ethylene diamine and self-assembled gold nanoparticle monolayers. Anal Chim Acta 2009;647:159–66.
[29] Joo J, Yim C, Kwon D, Lee J, Shin HH, Cha HJ, Jeon S. A facile and sensitive detection of pathogenic bacteria using magnetic nanoparticles and optical nanocrystal probes. Analyst 2012;137:3609–12.
[30] Jain S, Singh SR, Horn DW, Davis VA, Ram MJ, Pillai SR. Development of an antibody functionalized carbon nanotube biosensor for foodborne bacterial pathogens. J Biosens Bioelectron 2012;S11:002.
[31] Yang L, Li Y. Quantum dots as fluorescent labels for quantitative detection of *Salmonella typhimurium* in chicken carcass wash water. J Food Prot 2005;68:1241–5.
[32] Weeks BL, Camarero J, Noy A, Miller AE, Stanker L, De Yoreo JJ. A microcantilever-based pathogen detector. Scanning 2003;25:297–9.
[33] Grossman HL, Myers WR, Vreeland VJ, Bruehl R, Alper MD, Bertozzi CR, Clarke J. Detection of bacteria in suspension by using a superconducting quantum interference device. Proc Natl Acad Sci U S A 2004;101:129–34.
[34] Kaittanis C, Naser SA, Perez JM. One-step, nanoparticle-mediated bacterial detection with magnetic relaxation. Nano Lett 2007;7:380–3.
[35] Yakes BJ, Lipert RJ, Bannantine JP, Porter MD. Detection of *Mycobacterium avium* subsp. *paratuberculosis* by a sonicate immunoassay based on surface-enhanced Raman scattering. Clin Vaccine Immunol 2008;15:227–34.
[36] Li YS, Church JS. Raman spectroscopy in the analysis of food and pharmaceutical nanomaterials. J Food Drug Anal 2014;22:29–48.
[37] Norman RS, Stone JW, Gole A, Murphy CJ, Sabo-Attwood TL. Targeted photothermal lysis of the pathogenic bacteria, *Pseudomonas aeruginosa*, with gold nanorods. Nano Lett 2008;8:302–6.
[38] Zhao G, Xing F, Deng S. A disposable amperometric enzyme immunosensor for rapid detection of *Vibrio parahaemolyticus* in food based on agarose/nano-Au membrane and screen-printed electrode. Electrochem Commun 2007;9:1263–8.
[39] Zhao X, Hilliard LR, Mechery SJ, Wang Y, Bagwe RP, Jin S, Tan W. A rapid bioassay for single bacterial cell quantitation using bioconjugated nanoparticles. Proc Natl Acad Sci U S A 2004;101:15027–32.
[40] Phillips RL, Miranda OR, You CC, Rotello VM, Bunz UH. Rapid and efficient identification of bacteria using gold-nanoparticle-poly(*para*-phenyleneethynylene) constructs. Angew Chem Int Ed Engl 2008;47:2590–4.
[41] Huang YF, Wang YF, Yan XP. Amine-functionalized magnetic nanoparticles for rapid capture and removal of bacterial pathogens. Environ Sci Technol 2010;44:7908–13.
[42] Viswanathan S, Wu LC, Huang MR, Ho JA. Electrochemical immunosensor for cholera toxin using liposomes and poly(3,4-ethylenedioxythiophene)-coated carbon nanotubes. Anal Chem 2006;78:1115–21.
[43] Minke WE, Roach C, Hol WG, Verlinde CL. Structure-based exploration of the ganglioside GM1 binding sites of *Escherichia coli* heat-labile enterotoxin and cholera toxin for the discovery of receptor antagonists. Biochemistry 1999;38:5684–92.
[44] Schofield CL, Field RA, Russell DA. Glyconanoparticles for the colorimetric detection of cholera toxin. Anal Chem 2007;79:1356–61.
[45] Yang M, Kostov Y, Rasooly A. Carbon nanotubes based optical immunodetection of staphylococcal enterotoxin B (SEB) in food. Int J Food Microbiol 2008;127:78–83.
[46] Yang M, Kostov Y, Bruck HA, Rasooly A. Gold nanoparticle-based enhanced chemiluminescence immunosensor for detection of staphylococcal enterotoxin B (SEB) in food. Int J Food Microbiol 2009;133:265–71.
[47] Chien YY, Jan MD, Adak AK, Tzeng HC, Lin YP, Chen YJ, Wang KT, Chen CT, Chen CC, Lin CC. Globotriose-functionalized gold nanoparticles as multivalent probes for Shiga-like toxin. Chembiochem 2008;9:1100–9.
[48] Nagy JO, Zhang Y, Yi W, Liu X, Motari E, Song JC, Lejeune JT, Wang PG. Glycopolydiacetylene nanoparticles as a chromatic biosensor to detect Shiga-like toxin producing *Escherichia coli* O157:H7. Bioorg Med Chem Lett 2008;18:700–3.
[49] Uzawa H, Ohga K, Shinozaki Y, Ohsawa I, Nagatsuka T, Seto Y, Nishida Y. A novel sugar-probe biosensor for the deadly plant proteinous toxin, ricin. Biosens Bioelectron 2008;24:929–33.
[50] Taylor JD, Phillips KS, Cheng Q. Microfluidic fabrication of addressable tethered lipid bilayer arrays and optimization using SPR with silane-derivatized nanoglassy substrates. Lab Chip 2007;7:927–30.
[51] Tang D, Tang J, Su B, Chen G. Gold nanoparticles-decorated amine-terminated poly(amidoamine) dendrimer for sensitive electrochemical immunoassay of brevetoxins in food samples. Biosens Bioelectron 2011;26:2090–6.
[52] Goldman ER, Clapp AR, Anderson GP, Uyeda HT, Mauro JM, Medintz IL, Mattoussi H. Multiplexed toxin analysis using four colors of quantum dot fluororeagents. Anal Chem 2004;76:684–8.

[53] Branen JR, Hass MJ, Douthit WC, Maki WC, Branen AL. Detection of *Escherichia coli* O157, *Salmonella enterica* serovar *typhimurium*, and staphylococcal enterotoxin B in a single sample using enzymatic bio-nanotransduction. J Food Prot 2007;70:841–50.
[54] Sato K, Hosokawa K, Maeda M. Rapid aggregation of gold nanoparticles induced by non-cross-linking DNA hybridization. J Am Chem Soc 2003;125:8102–3.
[55] Li H, Rothberg LJ. Label-free colorimetric detection of specific sequences in genomic DNA amplified by the polymerase chain reaction. J Am Chem Soc 2004;126:10958–61.
[56] Karmakar A, Zhang Q, Zhang Y. Neurotoxicity of nanoscale materials. J Food Drug Anal 2014;22:147–60.
[57] Wu H, Yin JJ, Wamer WG, Zeng M, Lo YM. Reactive oxygen species-related activities of nano-iron metal and nano-iron oxides. J Food Drug Anal 2014;22:86–94.
[58] He W, Liu Y, Wamer WG, Yin JJ. Electron spin resonance spectroscopy for the study of nanomaterial-mediated generation of reactive oxygen species. J Food Drug Anal 2014;22:49–63.
[59] He X, Aker WG, Leszczynski J, Hwang HM. Using a holistic approach to assess the impact of engineered nanomaterials inducing toxicity in aquatic systems. J Food Drug Anal 2014;22:128–46.
[60] McShan D, Ray PC, Yu H. Molecular toxicity mechanism of nanosilver. J Food Drug Anal 2014;22:116–27.
[61] Chen T, Yan J, Li Y. Genotoxicity of titanium dioxide nanoparticles. J Food Drug Anal 2014;22:95–104.
[62] Li M, Yin JJ, Wamer WG, Lo M. Mechanistic characterization of titanium dioxide nanoparticle-induced toxicity using electron spin resonance. J Food Drug Anal 2014;22:76–85.
[63] United States Department of Homeland Security. BioWatch: Lessons learned and the path forward. Available from: http://www.dhs.gov/news/2014/06/10/written-testimony-oha-acting-assistant-secretary-and-st-under-secretary-house/ [Last accessed 21.04.15].